Review Article

Qiang Yue, Qiao Wang*, Timon Rabczuk, Wei Zhou, Xiaolin Chang, and Xiaoying Zhuang*

A review on modeling of graphene and associated nanostructures reinforced concrete

https://doi.org/10.1515/ntrev-2024-0033
received February 5, 2024; accepted April 30, 2024

Abstract: Concrete is the most popular construction material in infrastructure projects due to its numerous natural advantages. Nevertheless, concrete constructions frequently suffer from low tensile strength and poor durability performance which are always urgent tasks to be solved. The concrete reinforced by various nanomaterials, especially graphene and its associated nanostructures (GANS), shows excellent chemical and physical properties for engineering applications. The influence of GANS on cement composites is a multiscale behavior from the nanoscale to the macroscale, which requires a number of efforts to reveal *via* numerical and experimental approaches. To meet this need, this study provides a comprehensive overview of the numerical modeling for GANS reinforced concrete in various scales. The background and importance of the topic are addressed in this study, along with the review of its methodologies, findings, and applications. Moreover, the study critically summarizes the performance of GANS reinforced concrete, including its mechanical behavior, transport phenomena, and failure mechanism. Additionally, the primary challenges and future prospects in the research field are also discussed. By presenting an extensive overview, this review offers valuable insights for researchers and practitioners interested in numerical simulation to advance concrete science and engineering.

Keywords: graphene, cement composites, concrete, numerical modeling, multiscale behavior

*** Corresponding author: Qiao Wang,** State Key Laboratory of Water Resources Engineering and Management, Wuhan University, Wuhan, Hubei 430072, China; Institute of Water Engineering Sciences, Wuhan University, Wuhan, 430072, China, e-mail: qiaowang@whu.edu.cn
*** Corresponding author: Xiaoying Zhuang,** Institute of Photonics, Department of Mathematics and Physics, Leibniz University Hannover, Hannover, 30167, Germany, e-mail: zhuang@iop.uni-hannover.de
Qiang Yue: State Key Laboratory of Water Resources Engineering and Management, Wuhan University, Wuhan, Hubei 430072, China; Institute of Water Engineering Sciences, Wuhan University, Wuhan, 430072, China; Institute of Structural Mechanics, Bauhaus University Weimar, Weimar, 99423, Germany; Institute of Photonics, Department of Mathematics and Physics, Leibniz University Hannover, Hannover, 30167, Germany
Timon Rabczuk: Institute of Structural Mechanics, Bauhaus University Weimar, Weimar, 99423, Germany
Wei Zhou, Xiaolin Chang: State Key Laboratory of Water Resources Engineering and Management, Wuhan University, Wuhan, Hubei 430072, China; Institute of Water Engineering Sciences, Wuhan University, Wuhan, 430072, China

1 Introduction

Due to its numerous advantages, such as low-cost manufacture, easy shapeability, strong bonding power, and high compressive strength, concrete has become one of the most widely used building materials in civil and hydraulic engineering in the whole world [1]. However, the drawbacks of conventional concrete, including its weak corrosion resistance, poor tensile strength, and intrinsic brittleness, remain main issues to be overcome in engineering structures. For the purpose of improving the performance of cement composites, numerous attempts have been made to introduce various materials and techniques into the concrete, such as chemical admixtures, supplementary cementitious materials, surface coating materials, and fibers. It has been proven that advanced nanotechnology makes it possible to control the nano-sized defects (pores smaller than 20 nm in size) before micro-sized crack propagation. Consequently, nanomaterials like nano-titanium, nano-clay, nano-silica, and dioxide were studied as additions to concrete in many works [2,3]. Over the past years, graphene and its associated nanostructures (GANS) have become the new stars of carbon-based nanomaterials that can be incorporated into concrete owing to their extraordinary physical characteristics, *e.g.*, the specific surface area (2,630 $m^2\ g^{-1}$), tensile strength (130 GPa), Young's modulus (1.1 TPa), electronic mobility ($2 \times 10^5\ cm^2\ V^{-1}\ s^{-1}$), and thermal conductivity (~5,000 $W\ m^{-1}\ K^{-1}$) [4–7].

Graphene [8], which can be presented in a variety of shapes, is a single-layer carbon sheet with a two-dimensional honeycomb lattice nanostructure, as illustrated in Figure 1. In order to meet different requirements, graphene can be obtained in several chemical forms, including graphene nano platelets (GNP) [9], graphene oxide (GO) [10],

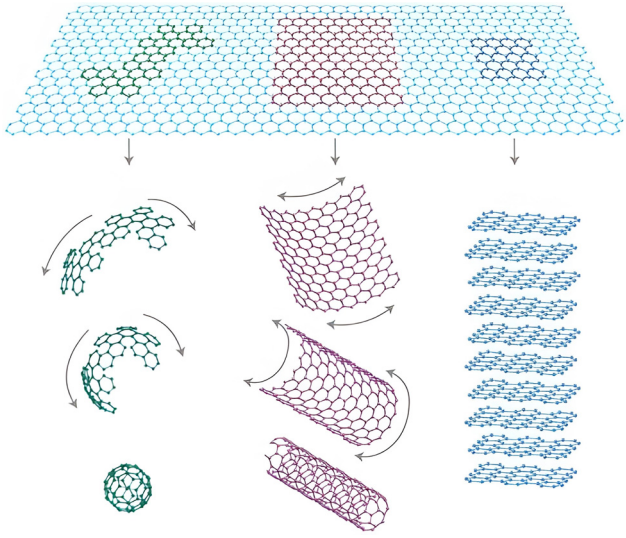

Figure 1: Graphene is a 2D basic material which can be reshaped to carbon materials of all other dimensionalities, including 0D buckyballs, 1D nanotubes, and 3D graphite [24].

graphene flakes [11], and reduced graphene oxide (rGO) [12]. Further, GANS can also be recognized as various materials according to their geometries and stacking modes, such as carbon nanotubes (CNT) [13], carbon nanofibers (CNF) [14], carbon nanocoil (CNC) [15], carbon black [16], carbon nanocone [17], graphene nanoribbons [18], graphene nanoislands [19], graphane [20], graphyne [21], and pristine graphene itself. Among the materials, several types of GANS like GNP, GO, and CNT are commonly used in cementitious composites to enhance their physical performance [22,23].

Practically, as one of the most often employed nanostructures in graphene reinforced concrete, GNP is a sheet-like material that can be readily produced from graphite or graphite oxide. It has a thickness of 3–100 nm and consists of several layers of graphene. Hence, GNP is a significant reinforcing material because of its morphological structure. GO is a layered material oxidized from graphite, with various oxygen-containing hydrophilic functional groups interspersed on the edges and basal surfaces of graphene. It has been proven that GO can effectively enhance the durability as well as mechanical performance of cement composites [25]. The main distinction between GNPs and GO for concrete depends on their electrical properties and dispersibility potential. In comparison to GNPs, GO is easier to disperse in water because of the oxygen groups on its sheet. However, the oxygen groups also make GO become an electrical insulator and lose advanced capabilities such as self-sensing. CNT, which is thought to be a good alternative to traditional reinforced fibers, is another popular research field in cement composites. It can be considered a cylinder obtained through rolling two-dimensional graphene layers. Besides, CNT can be classified into three types according to the number of walls, *i.e.*, single-walled CNT (SWCNT) [26], double-walled CNT [27], and multi-walled CNT [28]. Danoglidis *et al.* [29] found that the employment of CNTs significantly improves the mechanical performance of cement-based composites.

Researchers have noticed that many properties of concrete can be improved by incorporating graphene sheets into the composite. Pan *et al.* [30] concluded that adding 0.03% GO by cement weight to the cement paste can, respectively, increase the flexure, tensile, and compressive strengths of cement by 60.7, 78.6, and 38.9%. Jing *et al.* [31] found that when loading 0.2 and 0.4% graphene by weight of cement, the flowability of cement mortar can be diminished by 17.4 and 39%, respectively. According to the work of Wang *et al.* [32], evenly dispersed graphene can decrease the cement's stress under external loading and thus improve the strength properties of the cement composite. However, excessive graphene can lead to a degradation of physical properties due to the defects on the interface of different materials. Qureshi and Panesar [33] indicated that concrete's flexural and compressive strengths are best improved at 0.02 wt% graphene, whereas a larger concentration of graphene steadily degrades the performance of cement paste.

The heterogeneity of composite materials manifests itself at different scales, especially for cement-based materials with complex components [34,35]. To study the mechanical performance of GANS reinforced concrete, one can divide its internal structure into four levels, as depicted in Figure 2. According to the spatial scale, the four levels correspond to the macroscale (>10^{-1} m), mesoscale (10^{-3}–10^{-1} m), microscale (10^{-6}–10^{-4} m), and nanoscale (<10^{-6} m), respectively. At the nanoscale, the molecular structure of the calcium silicate hydrate (CSH) matrix and its connections with GANS can be considered. As one of the main hydration products at early

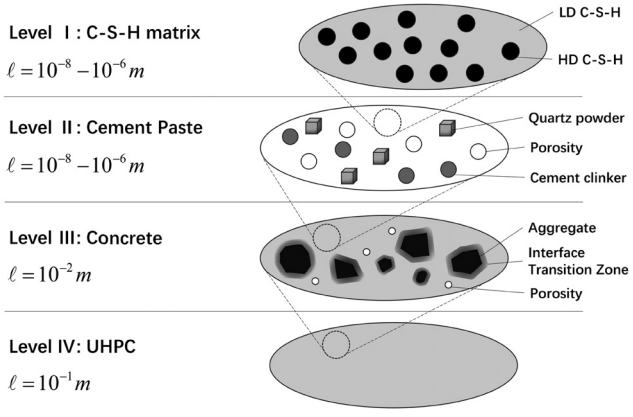

Figure 2: Four levels of the spatial scale for ultra-high-performance concrete.

ages, CSH significantly affects the mechanical behaviors of concrete. Further, the CSH matrix, together with the large portlandite crystals, aluminates, unhydrated cement products, and other cement compositions, forms the cement paste at the microscale. As for the mesoscale, concrete can be regarded as a three-phase composite material that is made up of aggregates, a cement paste matrix, and an interfacial transition zone connecting them. The highest level refers to continuous homogeneous materials. More precisely, the mechanical response of concrete is studied without considering the distribution of internal components, and the equivalent parameters obtained from homogenization approaches are used at the macroscale.

In this review, a thorough study on the numerical simulation of GANS reinforced concrete is performed. In Section 2, the modeling methods and their performance for GANS reinforced concrete in nano and micro scales are discussed. Then, the numerical aspects of GANS in cementitious composites from the meso and macro perspectives are presented in Section 3. Section 4 is devoted to the multiscale modeling strategies for GANS reinforced concrete. Finally, the concluding remarks and future prospects are given in Section 5.

2 Nanoscale and microscale performance of graphene reinforced concrete

2.1 Numerical models for CSH and GANS

The numerical analysis on atomic and molecular scales is typically based on the empirical force field methods or the quantum mechanics approaches. The quantum mechanics simulation methods, which can describe the electron motion accurately, are a type of techniques for modeling quantum mechanics using computer technology. Molecular mechanics (MD) is a rapidly developing theory based on empirical force fields as well as the Born-Oppenheimer approximation. The effects of electrons are neglected in the MD, and the function of nuclear coordinates is applied to express the energy of the system. It makes the MD more applicable for the modeling of larger systems, such as Monte Carlo [36], molecular statics [37], molecular dynamics [38], and so on.

As an analytical method at the nanometer scale, MD is the most important and frequently adopted theory due to its accuracy and flexibility. It combines computer technology, physics, chemistry, and mathematics to analyze the motion of molecular systems using Newtonian classical mechanics. In the past 20 years, MD simulation of CSH has been continuously improved to help study the structures, evolution, as well as other characteristics of hydrated cement matrix at the level of molecules [39]. The selection of the force field, which is built for representing the atom interactions, lies at the heart of MD simulation. For decades, hundreds of empirical force fields, which were validated with experimental data, have been developed for different research fields. Among them, some force fields are commonly applied to model cementitious composites, such as the consistent valence force field (CVFF), interface force field (IFF), COMPASS, CSH-FF, and so on. More details about the force fields can be found in Table 1.

2.2 Microscale mechanical properties and performance of GANS reinforced cement

GANS, whose sizes range from nanometers to micrometers, can dramatically impact the chemical and physical properties of hydrated cement composites, including chemical reactivity, heat conduction, strength, shrinkage, and creep [63–68]. In recent years, extensive works have been made to study the interactions between GANS and cement paste in cement hydrates, for example, molecular binding modes and hydration reaction rate [69,70]. The selected MD simulation investigations on the structures and performance of GANS-cement systems are summarized in Table 2. Based on the molecular modeling, Fan *et al.* [71] studied the shear strength of Go/cement interface. The result showed that the shear strength was 647.58 ± 91.18 MPa for the interface of GO cement, while 6–35 MPa for Portland cement. Wan and Zhang [72] compared the mechanical performance of ordinary Portland cement (OPC) and GO reinforced ultra-high performance concrete (UHPC), and explained the differences from the aspects of the structure, energies, and material properties of the CSH/GO interface. There are more hydroxyls and calcium dispersed in the interlayer for the CSH generated in UHPC, resulting in a larger interlayer spacing and more water absorption. The sites for the interfacial chemical bonds are occupied by hydroxyls and water, so that the Ca–O bonds and H-bond network at the CSH/GO interface are weakened. However, the water and hydroxyls play the role of bridges to connect GO sheet and CSH gel, as shown in Figure 3. Besides, the CSH/GO interface has a stronger tensile strength and larger interfacial interaction energy when there is more interlayer calcium for UHPC. Hou *et al.* [73] modeled the bonding properties of GO interfaced epoxy-concrete composite based on

Table 1: Popular force fields for cementitious systems

Force field	Basic features	Ref.
UFF	It is a full atomic force field that can be used for all elements in the periodic table	[40–42]
COMPASS	As a superior generalized ab initio force field, it is commonly applied in the modeling of liquids, polymers, and crystals	[43–45]
ClayFF	It is a force field designed for aqueous solution interfaces and hydrated multi-component mineral systems (mainly for clay-related phases). By treating most of the bonded interactions in the crystals as pseudo-ionic, the highly complex systems with millions of atoms are allowed for molecular simulations	[46,47]
CSH-FF	As a modified version of ClayFF, the force field is specially designed for CSH. Compared with other force fields such as ClayFF, it is more efficient for large systems due to the lower computational cost	[48–50]
IFF	It yields the consistency of inorganic and organic thermodynamics and is used in the simulation of the inorganic-organic interface. It is applicable for all kinds of elements and does not depend on quantum mechanical calculations of atomic charges	[51–53]
CVFF	It is a generalized valence force field that has been parameterized for water, various functional groups, and some inorganic materials, including silica	[25,54,55]
Cement-FF	All cementitious materials can be modeled with this force field. Potentials developed for similar atomic species systems are combined and adjusted in the model	[56]
Dreiding	This is a strictly diagonal force field possessing cosine-Fourier expansion torsion and harmonic valence terms. It can be used for a variety of structures	[40]
PCFF	The force field is originally created for organic and polymeric materials. Similar to COMPASS, it was parametrized for a number of functional groups	[52,57]
ReaxFF	It is a methodology between empirical force fields and quantum mechanics. In the modeling of chemical reactions and transition states, the force field employs bond order rather than fixed connections for chemical bonds	[58–60]
GB	It is originally established to express interactions between ellipsoidal particles and can be applied for controlling the interaction between the building blocks of disk-like CSH gel	[61,62]

molecular dynamics. The damage processes of epoxy-CSH and epoxy-GO-CSH systems under tension are compared in Figures 4 and 5. Obviously, the contact area on the interface of epoxy-GO-CSH system was considerably larger than that on epoxy-CSH system when they were under the same loading stage. It was concluded that the GO-modification of the epoxy/CSH interface can significantly increase its tensile resistance. The enhancement of bonding performance at epoxy-GO interfaces is due to the numerous hydrogen bonds that formed between GO's polar oxygen-containing functional groups and the epoxy molecules. When Go was coated on the polyethylene (PE) fiber, Lu *et al.* [74] observed a reduction in the translational motion of the atoms across the PE/CSH interface, which made the entire composite system more stable. The bonding energy at the CSH/GO as well as PE/GO interfaces is much higher compared to that at the weak CSH/epoxy interface, as illustrated in Figure 6. The topological structure and physical properties of the nanoscale additions, such as the connectivity and size distribution of pores in GANS, are also aspects that need to be considered in composite materials. The stochastic behaviors and effective material properties of functionally graded porous nanoscale plates are investigated by Tran *et al.* [75]. It was found that when the porosity density increases, the critical buckling loads decrease. For more details on this aspect, please refer to previous studies [76–78].

The transport properties, including ion diffusion and water permeability, can also be affected when cement is incorporated with GANS [79]. The influence of GNPs as well as graphene oxide nanoplatelets (GONPs) on the freeze-and-thaw properties of concrete was researched by Tong *et al.* [80] at the atomistic level. In their study, CSH-FF and ReaxFF were utilized to model the interatomic reactions of CSH gels. For the GONPs, the hydroxyl groups were described by using the harmonic bond potentials of O–H and C–O bonds, harmonic angular potentials of C–O–H and C–C–O angles, and harmonic dihedral potentials of C–C–O–H and C–C–C–O dihedral angles. Moreover, the OPLS-AA [81] force field for dialkyl ether was adopted to represent the epoxy groups. During the freeze/thaw cycles, the cyclic loads caused by pore water pressure in GNPs and GONPs reinforced concrete were 15.2 and 12 GPa higher than that in pure CSH gels, respectively. The graphene reinforced atomistic structures can increase the risk of nano-pore failure and worsen the freeze-and-thaw performance of concrete, especially for GNPs reinforced CSH gels. Zhao *et al.* [25] used molecular dynamics modeling and chloride diffusion tests to systematically study the transport behavior of GO reinforced cement. It was observed that the migration of chloride ions solution dramatically reduced when GO was introduced in the CSH pore. Due to the GO adsorbed on the inner surface of the CSH pore, the

Table 2: Summary of MD analyses on GANS reinforced concrete

Matrix	GNS type	Force field	Influence on	Highlights	Year	Ref.
CSH	GNPs; GONPs	ReaxFF; CSH-FF OPLS-AA	Freeze-and-thaw performance	The freeze-and-thaw performance of cement is compromised by the pure GNPs, whereas it can be improved by the GONPs	2016	[80]
CSH	CNT	Tersoff [82]	Mechanical properties	The addition of 2.351 Å CNT to the tobermorite with a diameter of 11 Å simultaneously improves its bulk modulus, shear modulus, and Young's modulus	2017	[83]
CSH	GO	COMPASS	Shear strength	The shear strength is 647.58 ± 91.18 MPa for CSH-GO interface, while 6–35 MPa for Portland cement at the macroscale	2017	[71]
CSH	GO	ReaxFF	Reactivity and interfacial bonding	In contrast to sulfate groups, carboxyl and hydroxyl groups can keep strong stability and prevent dissociation under the cement hydrate environment, making them ideal functional groups for reinforcing the GO/CSH composite	2018	[84]
PE-CSH	GO	ClayFF; CVFF	Shear strength	Comparing PE-GO-CSH to PE-CSH, the maximum pulling force for PE is enhanced by 41.67%; By enhancing the CSH-GO and PE-GO interfaces, which have higher interface binding energies than PE-CSH, GO can improve the strength of the weak PE-CSH interface	2020	[74]
CSH with NaCl solution	GO	ClayFF; CVFF	Durability	Because of the incorporation of GO sheets, the rate of ion and water migration in CSH is significantly lowered; The chloride ingress in cement can be restrained by the "immobilizing effect" and "caging effect" of GO sheets	2020	[25]
CSH	CNT	CSH-FF	Mechanical properties	CSH gains 100% more strength, 21% more elastic modulus, 70% more shear modulus, and 17% more bulk modulus after the addition of CNT (1.8%)	2020	[85]
CSH	CNT	COMPASSII [42]	Interaction	The binding ability of CNTs is not significantly affected by the number of walls; The strength of the interface is primarily determined by the type and amount of functional groups, as well as the relative orientation of the polar groups of CNT	2020	[86]
Epoxy-CSH	GO	ClayFF; CVFF	Tensile strength	The epoxy-GO-CSH interface has a much stronger tensile resistance than the epoxy-CSH interface because of the hydrogen bonds established between the epoxy molecules and the polar oxygen-containing functional groups of GO	2021	[73]
Concrete matrix	CNT	Lennard-Jones [87]	Poisson's ratio, Young's modulus	The mechanical properties of concrete samples with three different types of CNTs are compared and calculated	2021	[88]

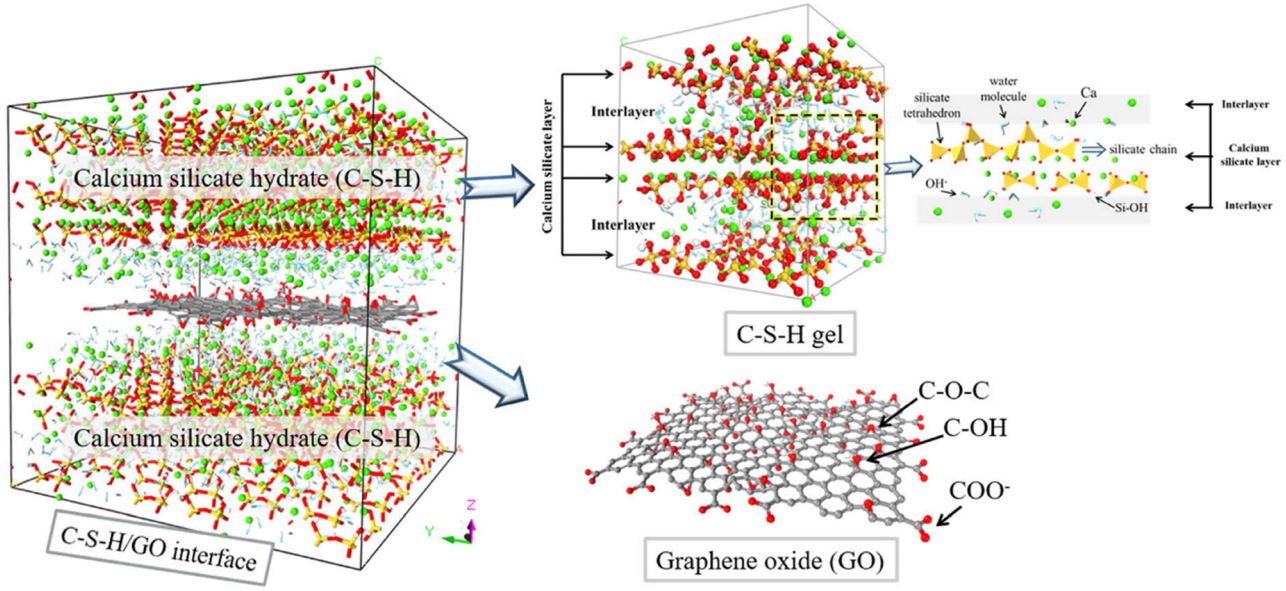

Figure 3: MD model for CSH gel and CSH/GO interface [72].

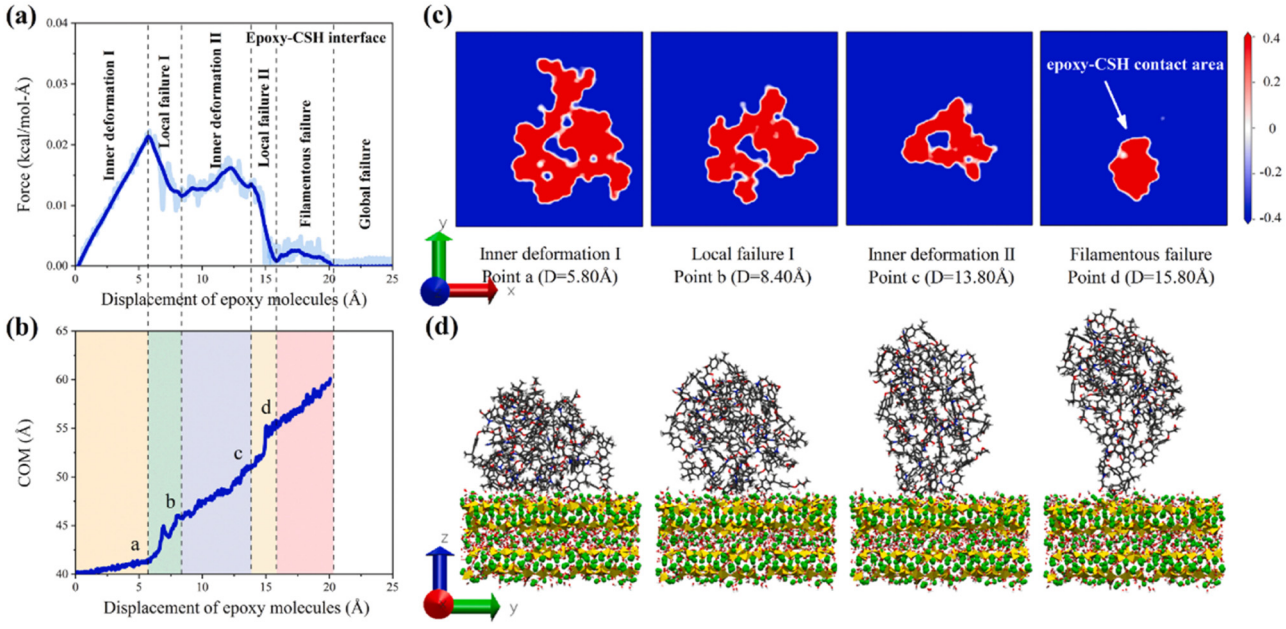

Figure 4: The performance of CSH-epoxy system at different loading stages: (a) load–displacement curve, (b) center of mass (COM) *vs* displacement curve for epoxy molecules, (c) CSH-epoxy contact area, and (d) simulation snapshots [73].

transportation of water can be hindered. As plotted in Figure 7, the solution species transportation in GO/CSH composite material is inhibited at the gel pore's entry point, while the pure CSH gel does not possess this capability.

Due to the excellent performance of GANS reinforced concrete, these type of materials have been widely applied in the fields of self-sensing, electromagnetic shielding, anti-corrosive coating, and so on [89–91]. It should be highlighted that the self-sensing and electromagnetic materials are themselves structural materials so that the overall structural performance would not be compromised by the traditional sensors. Moreover, it also shows great potential in the construction engineering which requires ultrahigh strength and durability of materials [92–94].

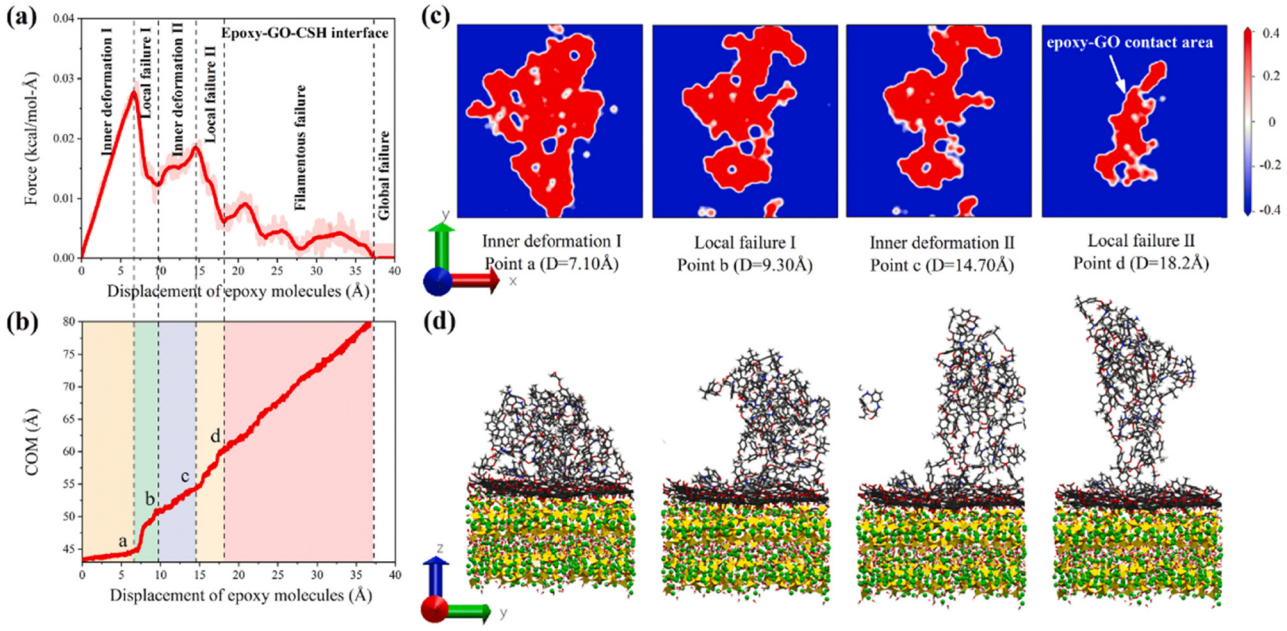

Figure 5: The performance of CSH-GO-epoxy system at different loading stages: (a) Load–displacement curve, (b) COM *vs* displacement curve for epoxy molecules, (c) CSH-epoxy contact area, and (d) simulation snapshots [73].

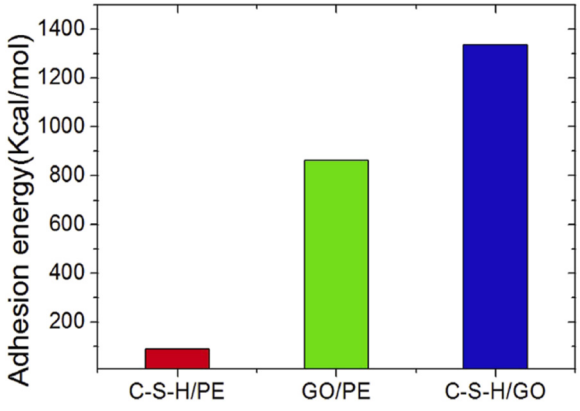

Figure 6: Adhesion energy of CSH/PE and CSH/GO/PE interfaces [74].

3 Mesoscale and macroscale performance of graphene reinforced concrete

3.1 Numerical methods for large-scale concrete

Although the microscale performance of GANS incorporated concrete has been studied by many researchers, it is quite necessary to develop the simulation at macro and mesoscales in practical engineering. During the decades, the mechanical behavior of concrete has been modeled by applying a series of numerical methods, for instance, the finite element method (FEM) [12,95,96], meshless method (MM) [97], discrete element method (DEM) [98], finite difference method (FDM) [99], peridynamics [100], differential quadrature method (DQM) [101], incremental harmonic balanced method [102], and boundary element method [103]. However, most of the published literature on modeling GANS reinforced concrete are based on the finite element simulation as a result of its wide applicability.

3.2 Mesoscale and macroscale simulation on GANS reinforced concrete

3.2.1 Research on getting material properties

The selection of precise material properties is crucial in the modeling of concrete [104]. There are two strategies commonly used to get the macroscale properties of concrete. The first method is measuring the results obtained from experiments [105], whereas another method is performing the equivalence using numerical simulation [106]. Anastopoulos *et al.* [107] compared two strategies, *i.e.*, the representative volume element (RVE) based homogenization method, and the multi-step homogenization method, to calculate the elastic properties of graphene-concrete composites, as depicted in Figure 8. In the method of multi-step homogenization, one can break the multi-phase composite into “grains,”

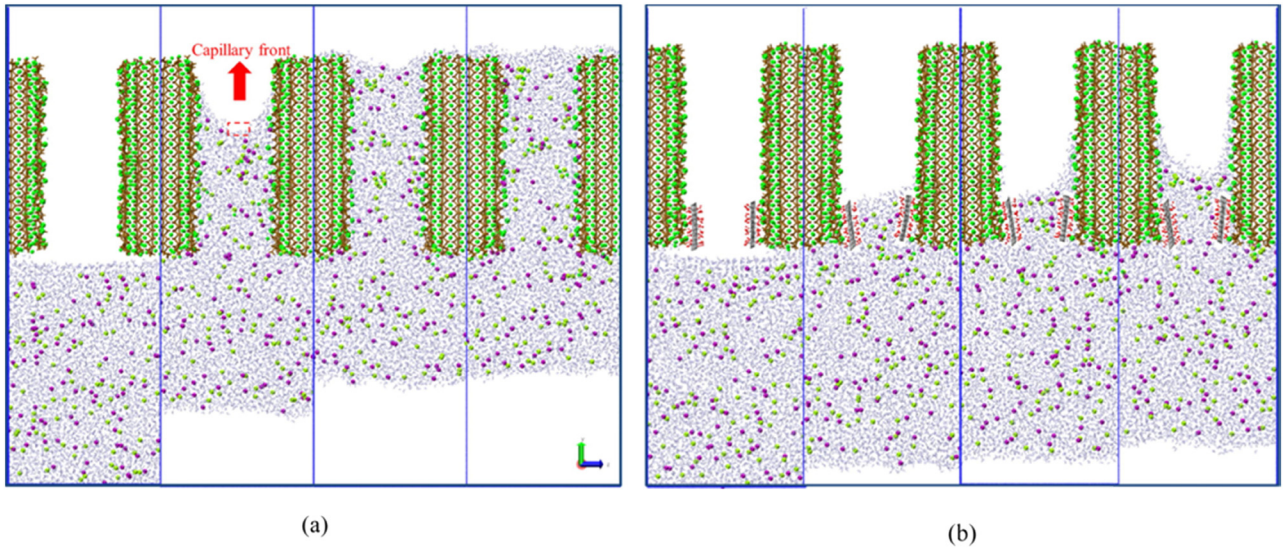

Figure 7: Translation of ions and water in the pore of (a) pure CSH gel, (b) CSH gel with incorporation of GO sheets (the white, gray, red, yellow, purple, and pale green balls represent hydrogen, carbon, oxygen, silicon, sodium, and chlorine atoms, respectively) [25].

with each grain composed of the matrix and one inclusion family. The same orientation, aspect ratio, and material properties are adopted for the inclusions of each family. Then, the Mori–Tanaka model and the Voigt formulation are applied in the homogenization process of the local grains and overall composite, respectively. For the RVE-based homogenization, the inclusions with random shapes and orientations are distributed in the element. The effective elastic properties of the composite can be obtained by modeling the RVE under tensile or shear loadings.

The electromagnetic parameters (complex permeability and complex permittivity) of GANS-based composites were studied by Santhosi *et al.* [108] using FEM. Compared to the conventional material, an improvement in microwave absorption was observed in composite concrete blocks. Le *et al.* [109] developed a mathematical model to estimate the damage extent in graphene reinforced concrete based on the measured fractional change in electrical resistance. This model was well verified by the physical experiments on the GNP-infused mortar.

3.2.2 Performance of GANS reinforced concrete

The cracking process of fiber-reinforced concrete embedded with graphene nanoplates was investigated by Pranno *et al.* [110,111]. It was noted that an increase in the absorbed energy by 20% and the first yielding load by 11% could be achieved for concrete when the volume fraction of graphene in concrete reached 0.1%, as shown in Figure 9. Besides,

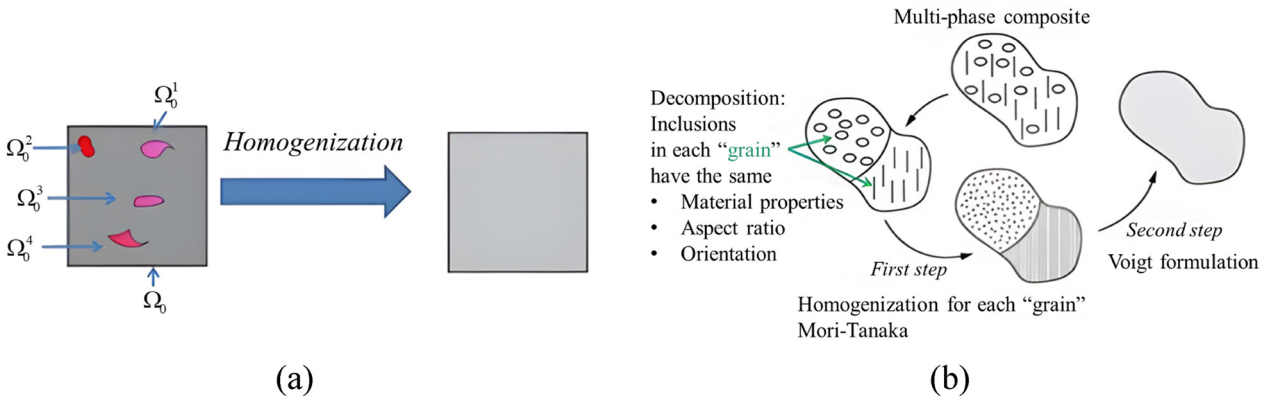

Figure 8: Homogenization methods of graphene-concrete composites [107]. (a) Representative volume element and (b) multi-step homogenization method reprentation.

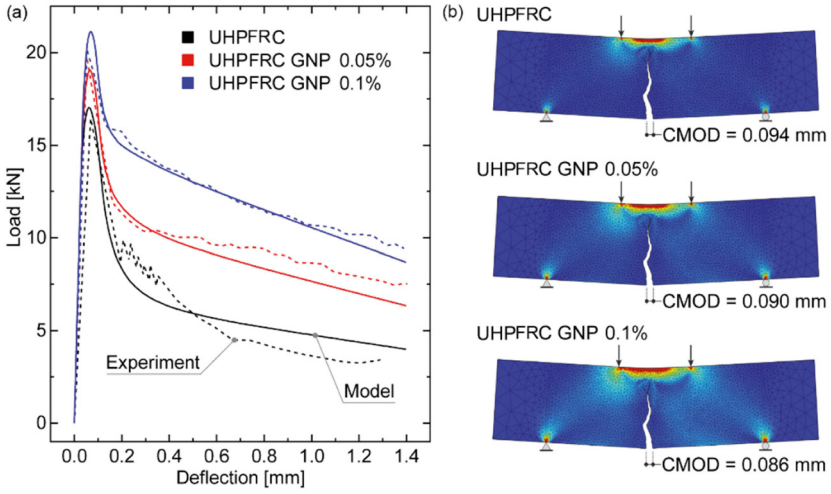

Figure 9: Comparison of cracking process of ultra-high-performance fiber-reinforced concrete (UHPFRC) with and without GNP: (a) load–deflection curves and (b) damage states [111].

Saeed [12] used FEM to model the influence of rGO on the damage in concrete which was induced by heat of hydration. By applying the mechanical properties measured from experiments, the temperature change and cracking index of rGO reinforced concrete was successfully reproduced. It was found that, when substituting 1.2% rGO for OPC, the cracking index of concrete could be reduced by decreasing the thermal gradient of the specimens.

In order to study the impact resistance of GO-modified rubberized engineered cementitious composite (GOCRECC), Abdulkadir *et al.* [112] discussed the influence of GO and crumb rubber (CR) on the initial and final impact energies of concrete. Based on the experimental data and response surface methodology (RSM), response-predictive models and optimization were proposed to get the impact resistance of similar materials. Similarly, Adamu *et al.* [113] employed RSM to examine how GNP and plastic waste (PW) affect the performance of concrete with high-volume fly ash (HVFA). The established model, which is in great agreement with experimental data, indicates that the optimal mix can be obtained by substituting 6.07% of cement with HVFA, 15.3% of coarse aggregate with PW, and adding GNP at 0.22%. Krystek *et al.* [114] verified the mechanical performance of graphene-based concrete *via* FE modeling based on the properties measured in laboratory tests. Acar *et al.* [115] focused on the influence of monolayer prepreg (MP) composites or graphene-reinforced monolayer prepreg (GMP) composites on the mechanical strengths of concrete beams. In accordance with the findings, credible solutions can be provided by MP and GMP composites for strengthening concrete structures. The buckling behavior of concrete columns armed with SWCNTs was investigated by Ali and Reza [116] based on DQM. Furthermore, the nonlinear buckling load grew gradually with the increase in volume percent of SWCNTs. Numerical results showed that the structure became stiffer when the concrete was reinforced by SWCNTs. The long-term performance of concrete, which is incorporated with carbon fiber reinforced polymer (CFRP) strips, was studied by Michele and Angelo [117]. The reinforcing strips were made of a polymer matrix incorporated with the long straight CNFs and CNTs, and their mechanical properties were assessed using a three-phase constitutive model. Additionally, two distinct creep functions were adopted to characterize the mechanical features of CFRP and concrete in the framework of linear viscoelasticity. More details about the mesoscale and macroscale modeling of GANS reinforced concrete can be found in Table 3.

4 Multiscale methodologies of GANS reinforced concrete

4.1 Multiscale models combining GANS with matrix

In order to precisely describe the physics of GANS based materials at various length scales, some researchers [125–128] proposed a series of coupling methods by combining MM/MD with FEM. Wei and Kysar [129] developed a multiscale method based on FEM to build the connections between macroscopic graphene membrane deformations with C–C interatomic behaviors. Then, many works [130–135] used the theory to model

Table 3: Summary of mesoscale and macroscale analyses on GANS reinforced concrete

Matrix	GNS type	Method	Influence on	Highlights	Year	Ref.
Cement	CNT	FEM	Constitutive behavior	To best enhance the structural ductility and strength of CNT reinforced concrete, the optimal combinations for interfacial and mechanical properties of CNT are searched	2009	[118]
Cement	CNT	FEM	Mechanical properties	It is found that the enhancement of CNT reinforced cement becomes stronger and then weaker with the continuous increase in the percentage of CNT	2012	[119]
Concrete	SWCNTs	DQM	Buckling behavior	An original model for the concrete column with SWCNT is proposed, in which the Timoshenko and Euler-Bernoulli beam models are employed	2016	[116]
Cement	CNTs	FEM	Fracture energy	The CNT-cement composite's size-independent fracture energy is determined using numerical analyses	2017	[120]
Cement	GO	Boundary nucleation-growth model (BNG)	Nucleation-growth during hydration	BNG [120] is used to mathematically describe the role of GO when it is regarded as a nucleation-growth site	2017	[121]
Concrete	GMP	FEM	Flexural strength and tensile strength	When MP was substituted with GMP in concrete, the results showed an improvement in the tensile strength of about 7% and the flexural strength of 1–3.7%	2017	[115]
UHPFRC	Fiber	DFEM	Failure modes	A discrete-continuum coupled finite element modeling method is developed to study the crushing, spalling, mortar cracking as well as fiber breakage behaviors of fiber reinforced concrete	2018	[122]
Concrete	CNT	FEM	Conductive properties	To simulate the CNT reinforced composites at an arbitrary strain state, a mixed micromechanics-FEM approach is presented	2018	[95]
Concrete	CFRP	FEM	Creep behavior	The influence of the number and thickness of CFRP strips, as well as the CNT mass fraction, are researched for the long-term behavior of concrete	2020	[117]
CRECC	GO	RSM	Impact resistance	The predictive models for initial and ultimate impact energy of GOCRECC are proposed. It is indicated that optimal amounts of GO and CR by cement weight added in the composite are 0.0347% and 5%, respectively	2021	[112]
HVFA concrete	GNP	RSM	Mechanical properties	For the strengths of HVFA concrete, the adverse effects of fly ash and PW can be significantly mitigated by adding GNP in the concrete	2021	[113]
Functionally graded composite beams	GO	MM	Bending behavior	A multiquadric radial basis function-based meshless collocation method is applied to assess the mechanical responses of GO powder reinforced functionally graded composite beams	2021	[97]
Mortar	rGO	FEM	Cracking index	The mechanical properties obtained from experiments are adopted to research how rGO affects the damage process of concrete due to temperature stress	2022	[12]
Concrete	Graphene flake	FEM	Microwave absorption	Compared with conventional concrete blocks, the concrete reinforced by graphene-based hybrid nanocomposites has a stronger capability in terms of microwave absorption	2022	[108]
UHPFRC	GNP	DIM	Fracture	The cohesive elements with a nonlinear traction-separation law are applied to model the initiation and evolution of the fracture. The enhancement on the force responses of UHPFRC, which results from the addition of graphene nanoparticles, can be successfully predicted by the model	2022	[123]
Concrete	CNTs	FDM	Electrical properties	The electrical conductivity of concrete, which is reinforced by randomly dispersed carbon fibers, can be determined by the model	2023	[124]

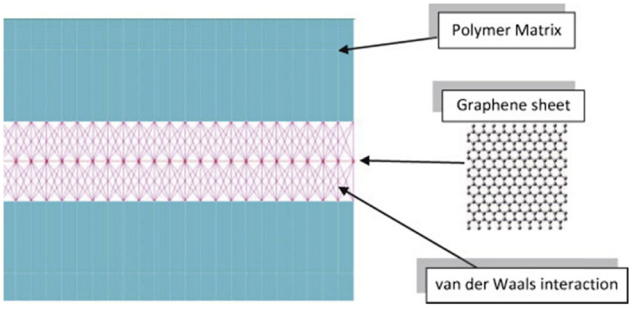

Figure 10: Multiscale model of graphene reinforced composites: Carbon atoms, covalent bonds, L–J potential, and the polymer matrix are represented by nodes, Timoshenko beams, truss elements, and 3D solid elements, respectively [138].

the multiscale behaviors of GANS based composite structures. However, it is still difficult to capture the nanoscale characteristics of all components (matrix, fiber, filler, interphase) of composites. For this reason, some literature [130,136–138] simplified the composite materials as a multiscale system, in which some components such as matrix as well as fibers were considered at the macro-scale level while the other constituents were modeled at the nanoscale level. Among the works, most of the simulations adopted strategies that involve representing GANS as a lattice frame structure. In the structure, GANS are discretized with one-dimensional truss elements, while the matrix is represented by the continuous three-dimensional solid elements. This method can also be called the unit cell method or RVE method [139], which is also introduced in Section 3.1. In the RVE, as shown in Figure 10, the GANS and the matrix can be connected using van der Waals interaction forces [138]. When the deflection exceeds a certain threshold, the interface bonds (truss elements) that connect GANS and the matrix can be removed. Apart from the spring element, various other types of elements have been developed to model carbon nanostructures and C–C bonds in GANS, which are applicable to different problems [128]. The elements for representing carbon nanostructures are summarized in Table 4.

Although the atomistic simulation and the beam finite elements can accurately characterize the structure of GANS, they are very time-consuming in the multiscale modeling. To solve this problem, a continuum mechanics surrogate model was proposed by Papadopoulos *et al.* [140] for the simulation of graphene. To reproduce the shell-type structural behavior of graphene platelets, the work presented an equivalent shell element as the substitute of the detailed molecular dynamics models for graphene. This shell finite element model of graphene is proven to be capable of effectively representing both its membrane and plate behaviors. As plotted in Figure 11, the features of the graphene particles, including the random wrinkling behavior, and the delamination and debonding phenomena, can be well simulated. Apart from the mentioned elements, various other types of elements have been developed to represent C–C bonds and

Table 4: Elements for representing C–C bonds and carbon nanostructures in GANS

Element type	Highlights	Structure	Ref.
CC-beams	It is a type of element that can model the C–C bonds' tension, bending, and torsion behaviors. It also has the benefits of simple implementation and high efficiency	Six beam elements are used to depict the hexagonal lattice of graphene	[141,142]
CC-springs	The geometrical properties of spring elements depend on the natural characteristics of C–C bonds. It is more suitable for modeling the nonlinear behavior of carbon nanostructures	The hexagonal is composed of 12 spring elements, wherein 6 elements simulate translations and the remaining 6 elements simulate angular variations	[143,144]
CC-TRF	The C–C bonds are modeled with truss, rod, and frame elements in the method	A hexagonal cell of graphene is also represented by 12 elements, where 6 elements are used for representing stretching while the remaining 6 elements are used to depict in-plane bending	[145]
2D-Elem	Two-dimensional elements such as plane strain, plane stress, and plate elements are adopted	—	[146,147]
Shell-Ele	Shell-type elements are applied to express the graphene-based nanostructures	—	[140,148–150]
3D-Ele	The nanostructure of GANS is represented by three-dimensional solid elements, for example, hexahedral and tetrahedral elements	—	[151–153]
Axisym-Elem	Axisymmetric elements are used in the model	—	[154,155]
Spec-Elem	Special-purpose elements are introduced to meet specific requirements	—	[156,157]

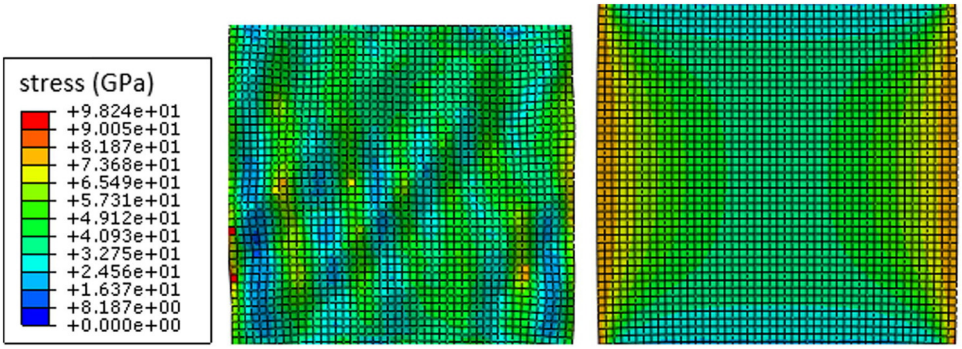

Figure 11: Tensile stress distributions on a single-layer graphene sheet: wrinkled (left) and straight (right) [140].

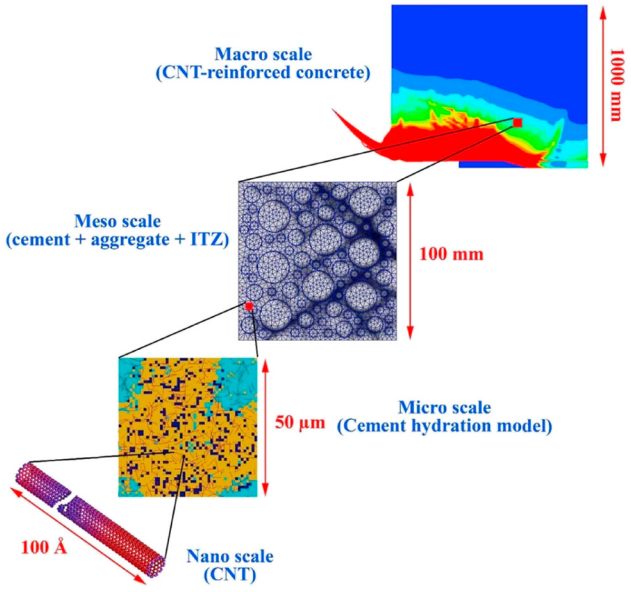

Figure 12: The multiscale simulation for the fracture of a CNT-reinforced concrete [158].

carbon nanostructures in GANS, which are applicable for different problems [128].

4.2 Multiscale models with multilevel equivalence

The properties of concrete at a higher scale depend on those of the components at a lower scale. Hence, many researches were devoted to revealing the mechanical response mechanisms of concrete from the nanoscale to the macroscale. As shown in Figure 12, Eftekhari and Mohammadi [158] explained the dynamic behaviors of CNT reinforced concrete from different scale perspectives, *i.e.*, nanoscale, microscale, mesoscale, and macroscale. On the nanoscale, the molecular structure of CNT was carefully modeled using the MD approach. Then, the mean values of the results obtained from nanoscale simulations were applied to the microscale modeling of CNT reinforced cement. Then, the microscale FE simulation was carried out based on a particle kinetics chemical hydration theory. When the properties of cement are determined, the mesoscale analysis of concrete can be implemented. Finally, based on the equivalent properties calculated from the numerical results at the mesoscale, the global mechanical behavior at the macroscale can be studied *via* FEM. This multiscale modeling strategy was also adopted by many other works [159–165] to investigate the influence of the added graphene-based nanomaterials on concrete. Moreover, the fracture behavior of the CNT reinforced concrete at the mesoscale was studied by Eftekhari *et al.* [13] with the aid of MD and RVE simulations. It was observed that a remarkable delay occurred in the initiation and propagation of mixed-mode fractures.

Similarly, Papadopoulos and Impraimakis [166] evaluated the nonlinear constitutive relationship of CNTs reinforced concrete using hierarchical RVEs, which were in accordance with the material's microstructural topology. As can be seen in Figure 13, several RVEs with different sizes were constructed in the hierarchical multiscale modeling strategy. The lowest nanoscale RVE1, which is initially resolved, only contains CNTs and the cement paste. The computational homogenization on the lower RVE can result in an equivalent "enhanced" cement paste, which is utilized in the higher RVE. Moreover, the aggregates of different dimensions (from 0.125 to 32 mm) can be considered in the corresponding RVEs. Based on the information passed through scales, both elastic and inelastic analyses of concrete can be performed on all scales.

Wang *et al.* [167] developed a multiscale modeling method involving the length-scale integration, and further verified its ability to obtain the effective properties by

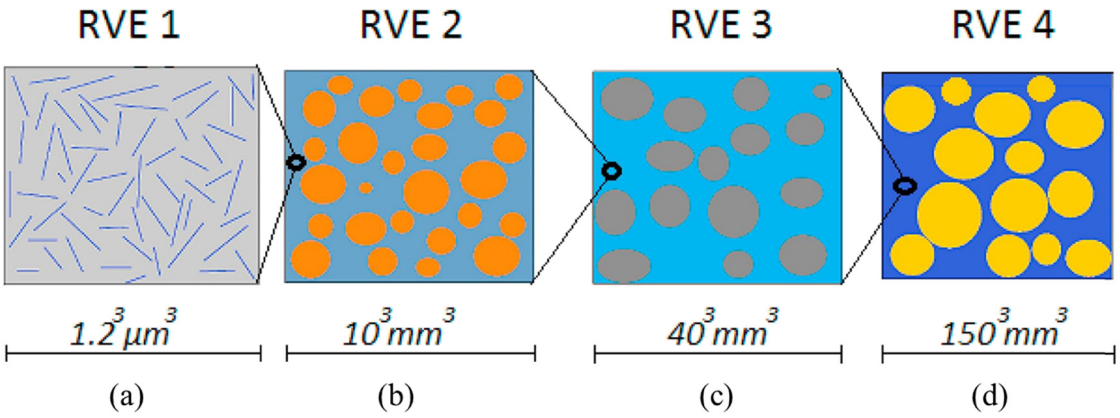

Figure 13: Hierarchical RVEs for cementitious composites with (a) RVE1 CNTs (RVE1), (b) aggregates smaller than 2 mm (RVE2), (c) aggregates smaller than 8 mm (RVE3), and (d) aggregates smaller than 32 mm (RVE4) [166].

upscaling. Based on this upscaling process, the properties of cement mortar can be estimated using Mori–Tanaka and self-consistent approaches [168]. Then, the meshless technique can be applied to estimate the material parameters of CNT reinforced cementitious composites at the macroscale.

4.3 Machine learning

With the development of machine learning, the technique began to be applied to the prediction of multiscale behaviors of concrete [169–172]. Lyngdoh and Das [173] combined machine learning (forward neural network) with a validated FEM-based multiscale modeling framework to estimate the strain-sensing performance of self-sensing concrete which is reinforced by nano-engineered materials. This model, as illustrated in Figure 14, showed excellent efficiency in the prediction of the electromechanical response. Lu *et al.* [174] also outlined a data-driven computational homogenization method that can be used in the simulation for the electrical responses of graphene-reinforced composites. The related works based on other machine learning techniques, such as deep convolutional neural network, fully convolutional network, and support vector machine, can be found in the previous literature [175–177].

5 Conclusion

In the present work, an extensive overview of the numerical modeling techniques and strategies for GANS reinforced concrete is presented. The numerical works considering the geometry characteristics, material properties, constitutive models, internal components of GANS reinforced concrete are discussed at different spatial scales. The following conclusions can be drawn based on the review:

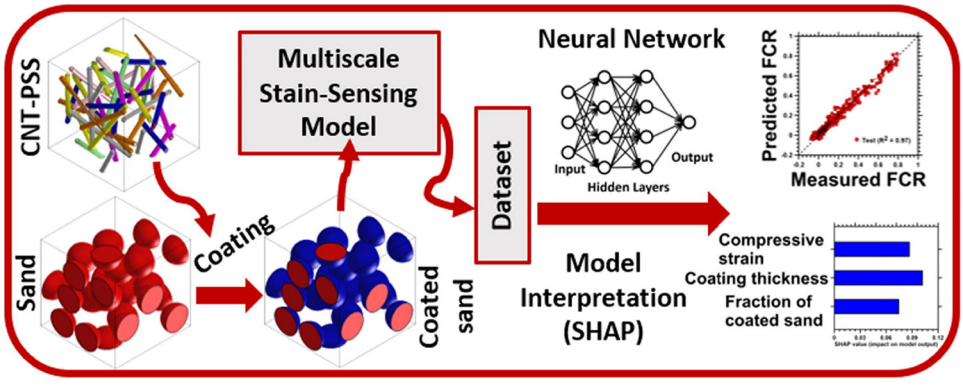

Figure 14: A technique combining multiscale numerical modeling with machine learning [173].

1) GANS reinforced concrete is a type of composites with complex performance at different scales. The addition of GANS has a significant influence on concrete in many aspects, including the mechanical behaviors, transport properties, and failure mechanisms. GANS have the potential to increase the bulk modulus, shear modulus, and Young's modulus of concrete, resulting in the larger strengths of concrete. Additionally, the durability of concrete can be improved by GANS by lowering the ion and water migration in CSH gel. The enhancement of GANS reinforced composites at the nanoscale and microscale is significantly greater compared to that at the macroscale, primarily attributed to defects present across multiple scales. Generally, the appropriate addition of GANS can lead to an improvement of the properties for concrete, while excessive GANS may cause harm to the cementitious composites.
2) In nanoscale and microscale modeling, the structure of cementitious composites can be generated using quantum mechanics and molecular dynamics methods. The interfacial bonding and mechanical performance of GANS reinforced cement can be predicted using MD simulation. The force fields developed for cementitious composites can be adopted to analyze the microscale behavior of GANS reinforced concrete. As for the mesoscale and macroscale modeling, many numerical methods can be used to study the material's physical and chemical performance, such as the FEM, meshfree method, and DEM. The equivalent properties of RVE obtained from physical experiments and homogenization strategies can be applied to understand the mechanical response mechanism of concrete at a large scale.
3) In the global simulation of concrete considering the distribution of GANS, a series of elements, such as the truss elements and beam elements, can be used as efficient and reliable tools to characterize the chemical bonds and nanostructures of GANS. Hence, multiscale modeling can be achieved in the framework of FEM. Another multiscale modeling strategy is passing the material parameters between the RVEs at different levels. It helps to understand the performance of concrete at all scales and the relationships between material parameters at different scales. Moreover, machine learning has become a popular mode to study the multiscale response of GANS incorporated concrete. Nevertheless, very limited research was devoted on the multiscale performance of GANS reinforced concrete. More efficient and accurate models need to be developed to reveal the effects of GANS on the macroscale response of concrete structure.

In conclusion, GANS can drive the enhancement of cementitious materials and support the development of construction industry. Moreover, numerical modeling can help in the design and optimization of GANS reinforced cementitious materials, by providing a thorough understanding of their mechanical, structural, and transport properties. The introduction of GANS into concrete production provides a pathway for a more substantial future and great opportunities for construction engineering.

Acknowledgements: Financial support by the National Key R&D Program of China (No. 2022YFC3005505) and the National Natural Science Foundation of China (Nos U2040223 and 51979207), is gratefully acknowledged.

Funding information: The National Key R&D Program of China (No. 2022YFC3005505) and the National Natural Science Foundation of China (Nos U2040223 and 51979207).

Author contributions: All authors have accepted responsibility for the entire content of this manuscript and approved its submission.

Conflict of interest: The authors state no conflict of interest.

Data availability statement: All data generated or analysed during this study are included in this published article.

References

[1] Chanut N, Stefaniuk D, Weaver JC, Zhu Y, Shao-Horn Y, Masic A, et al. Carbon–cement supercapacitors as a scalable bulk energy storage solution. Proc Natl Acad Sci. 2023;120:e2304318120.
[2] Kashif Ur Rehman S, Kumarova S, Ali Memon S, Javed MF, Jameel M. A review of microscale, rheological, mechanical, thermoelectrical and piezoresistive properties of graphene based cement composite. 2020;10:2076.
[3] Zhong R, Zhang F, Poh LH, Wang S, Le HTN, Zhang M-H. Assessing the effectiveness of UHPFRC, FRHSC and ECC against high velocity projectile impact. Cem Concr Compos. 2021;120:104013.
[4] Balandin AA, Ghosh S, Bao W, Calizo I, Teweldebrhan D, Miao F, et al. Superior thermal conductivity of single-layer graphene. Nano Lett. 2008;8:902–7.
[5] Lee C, Wei X, Kysar JW, Hone J. Measurement of the elastic properties and intrinsic strength of monolayer graphene. Science. 2008;321:385–8.
[6] Bolotin KI, Sikes KJ, Jiang Z, Klima M, Fudenberg G, Hone J, et al. Ultrahigh electron mobility in suspended graphene. Solid State Commun. 2008;146:351–5.
[7] Stoller MD, Park S, Zhu Y, An J, Ruoff RS. Graphene-based ultracapacitors. Nano Lett. 2008;8:3498–502.
[8] Mohan VB, Lau K-t, Hui D, Bhattacharyya D. Graphene-based materials and their composites: A review on production, applications and product limitations. Compos Part B: Eng. 2018;142:200–20.

[9] Young RJ, Liu M, Kinloch IA, Li S, Zhao X, Vallés C, et al. The mechanics of reinforcement of polymers by graphene nanoplatelets. Compos Sci Technol. 2018;154:110–6.
[10] Habibnejad Korayem A, Ghoddousi P, Shirzadi Javid AA, Oraie MA, Ashegh H. Graphene oxide for surface treatment of concrete: A novel method to protect concrete. Constr Build Mater. 2020;243:118229.
[11] Low CTJ, Walsh FC, Chakrabarti MH, Hashim MA, Hussain MA. Electrochemical approaches to the production of graphene flakes and their potential applications. Carbon. 2013;54:1–21.
[12] Saeed M. Three-dimensional finite element modelling for influence of reduced graphene oxide on cracking index of mass mortar blocks due to heat of hydration. Aust J Civ Eng. 2023;21:194–206.
[13] Eftekhari M, Hatefi Ardakani S, Mohammadi S. An XFEM multiscale approach for fracture analysis of carbon nanotube reinforced concrete. Theor Appl Fract Mech. 2014;72:64–75.
[14] Sanchez F, Zhang L, Ince C. Multi-scale performance and durability of carbon nanofiber/cement composites. In: Bittnar Z, Bartos PJM, Němeček J, Šmilauer V, Zeman J, editors. Nanotechnology in Construction Vol. 3. Berlin, Heidelberg: Springer Berlin Heidelberg; 2009. p. 345–50.
[15] Chen X, Zhang S, Dikin DA, Ding W, Ruoff RS, Pan L et al. Mechanics of a carbon nanocoil. Nano Lett. 2003;3:1299–304.
[16] Ding Y, Chen Z, Han Z, Zhang Y, Pacheco-Torgal F. Nano-carbon black and carbon fiber as conductive materials for the diagnosing of the damage of concrete beam. Constr Build Mater. 2013;43:233–41.
[17] Yang N, Zhang G, Li B. Carbon nanocone: A promising thermal rectifier. Appl Phys Lett. 2008;93:243111.
[18] Celis A, Nair MN, Taleb-Ibrahimi A, Conrad EH, Berger C, de Heer WA, et al. Graphene nanoribbons: fabrication, properties and devices. J Phys D: Appl Phys. 2016;49:143001.
[19] Fernández-Rossier J, Palacios JJ. Magnetism in graphene nanoislands. Phys Rev Lett. 2007;99:177204.
[20] Sofo JO, Chaudhari AS, Barber GD. Graphane: A two-dimensional hydrocarbon. Phys Rev B. 2007;75:153401.
[21] Cranford SW, Buehler MJ. Mechanical properties of graphyne. Carbon. 2011;49:4111–21.
[22] Konsta-Gdoutos MS, Metaxa ZS, Shah SP. Carbon nanotubes reinforced concrete. Special Publication. 2009;267:11–20.
[23] Chuah S, Pan Z, Sanjayan JG, Wang CM, Duan WH. Nano reinforced cement and concrete composites and new perspective from graphene oxide. Constr Build Mater. 2014;73:113–24.
[24] Geim AK, Novoselov KS. The rise of graphene. Nat Mater. 2007;6:183–91.
[25] Zhao L, Hou D, Wang P, Guo X, Zhang Y, Liu J, et al. Experimental and molecular dynamics studies on the durability of sustainable cement-based composites: Reinforced by graphene. Constr Build Mater. 2020;257:119566.
[26] Makar J. The effect of SWCNT and other nanomaterials on cement hydration and reinforcement. In: Gopalakrishnan K, Birgisson B, Taylor P, Attoh-Okine NO, editors. Nanotechnology in Civil Infrastructure: A Paradigm Shift. Berlin, Heidelberg: Springer Berlin Heidelberg; 2011. p. 103–30.
[27] Al-Zu'bi M, Fan M, Anguilano L. Advances in bonding agents for retrofitting concrete structures with fibre reinforced polymer materials: A review. Constr Build Mater. 2022;330:127115.
[28] Choi H, Kang D, Seo GS, Chung W. Effect of some parameters on the compressive strength of MWCNT-cement composites. Adv Mater Sci Eng. 2015;2015:340808.
[29] Danoglidis PA, Konsta-Gdoutos MS, Gdoutos EE, Shah SP. Strength, energy absorption capability and self-sensing properties of multifunctional carbon nanotube reinforced mortars. Constr Build Mater. 2016;120:265–74.
[30] Pan Z, He L, Qiu L, Korayem AH, Li G, Zhu JW, et al. Mechanical properties and microstructure of a graphene oxide–cement composite. Cem Concr Compos. 2015;58:140–7.
[31] Jing G, Ye Z, Lu X, Hou P. Effect of graphene nanoplatelets on hydration behaviour of Portland cement by thermal analysis. 2017;29:63–70.
[32] Wang B, Jiang R, Wu Z. Investigation of the mechanical properties and microstructure of graphene nanoplatelet-cement composite. Nanomaterials. 2016;6(11):200.
[33] Qureshi TS, Panesar DK. Nano reinforced cement paste composite with functionalized graphene and pristine graphene nanoplatelets. Compos Part B: Eng. 2020;197:108063.
[34] Sorelli L, Constantinides G, Ulm F-J, Toutlemonde F. The nano-mechanical signature of ultra high performance concrete by statistical nanoindentation techniques. Cem Concr Res. 2008;38:1447–56.
[35] Bernard O, Ulm F-J, Lemarchand E. A multiscale micromechanics-hydration model for the early-age elastic properties of cement-based materials. Cem Concr Res. 2003;33:1293–1309.
[36] Hou D, Zhang J, Li Z, Zhu Y. Uniaxial tension study of calcium silicate hydrate (C–S–H): structure, dynamics and mechanical properties. Mater Struct. 2015;48:3811–24.
[37] Palkovic SD, Yip S, Büyüköztürk O. Constitutive response of calcium-silicate-hydrate layers under combined loading. J Am Ceram Soc. 2017;100:713–23.
[38] Yu J, Hou D, Ma H, Wang P. Nanomodified cement-based materials: review (2015–2020) of molecular dynamics studies. J Mater Civ Eng. 2022;34:03121002.
[39] Cho BH, Chung W, Nam BH. Molecular dynamics simulation of calcium-silicate-hydrate for nano-engineered cement composites – a review. 2020;10:2158.
[40] Wu W, Al-Ostaz A, Cheng Alexander HD, Song Chung R. Computation of elastic properties of portland cement using molecular dynamics. J Micromech Microeng. 2011;1:84–90.
[41] Tavakoli D, Tarighat A. Molecular dynamics study on the mechanical properties of Portland cement clinker phases. Comput Mater Sci. 2016;119:65–73.
[42] Al-Ostaz A, Wu W, Cheng AHD, Song CR. A molecular dynamics and microporomechanics study on the mechanical properties of major constituents of hydrated cement. Compos Part B: Eng. 2010;41:543–9.
[43] Du J, Bu Y, Shen Z. Interfacial properties and nanostructural characteristics of epoxy resin in cement matrix. Constr Build Mater. 2018;164:103–12.
[44] Hajilar S, Shafei B. Nano-scale investigation of elastic properties of hydrated cement paste constituents using molecular dynamics simulations. Comput Mater Sci. 2015;101:216–26.
[45] Shu X, Ran Q, Liu J, Zhao H, Zhang Q, Wang X, et al. Tailoring the solution conformation of polycarboxylate superplasticizer toward the improvement of dispersing performance in cement paste. Constr Build Mater. 2016;116:289–98.
[46] Fu J, Bernard F, Kamali-Bernard S. Assessment of the elastic properties of amorphous calcium silicates hydrates (I) and (II) structures by molecular dynamics simulation. Mol Simul. 2018;44:285–99.

[47] Cygan RT, Liang J-J, Kalinichev AG. Molecular models of hydroxide, oxyhydroxide, and clay phases and the development of a general force field. J Phys Chem B. 2004;108:1255–66.
[48] Hou D, Yu J, Wang P. Molecular dynamics modeling of the structure, dynamics, energetics and mechanical properties of cement-polymer nanocomposite. Compos Part B: Eng. 2019;162:433–44.
[49] Shahsavari R, Pellenq RJM, Ulm F-J. Empirical force fields for complex hydrated calcio-silicate layered materials. Phys Chem Chem Phys. 2011;13:1002–11.
[50] Hou D, Li H, Zhang L, Zhang J. Nano-scale mechanical properties investigation of C-S-H from hydrated tri-calcium silicate by nano-indentation and molecular dynamics simulation. Constr Build Mater. 2018;189:265–75.
[51] Heinz H, Lin T-J, Kishore Mishra R, Emami FS. Thermodynamically consistent force fields for the assembly of inorganic, organic, and biological nanostructures: the interface force field. Langmuir. 2013;29:1754–65.
[52] Chaudhari O, Biernacki JJ, Northrup S. Effect of carboxylic and hydroxycarboxylic acids on cement hydration: experimental and molecular modeling study. J Mater Sci. 2017;52:13719–35.
[53] Mishra RK, Fernández-Carrasco L, Flatt RJ, Heinz HJDT. A force field for tricalcium aluminate to characterize surface properties, initial hydration, and organically modified interfaces in atomic resolution. 2014;43:10602–16.
[54] Zhou Y, Hou D, Jiang J, She W, Li J. Molecular dynamics study of solvated aniline and ethylene glycol monomers confined in calcium silicate nanochannels: a case study of tobermorite. Phys Chem Chem Phys. 2017;19:15145–59.
[55] Zhou Y, Tang L, Liu J, Miao C. Interaction mechanisms between organic and inorganic phases in calcium silicate hydrates/poly (vinyl alcohol) composites. Cem Concr Res. 2019;125:105891.
[56] Mishra RK, Mohamed AK, Geissbühler D, Manzano H, Jamil T, Shahsavari R, et al. Cemff: A force field database for cementitious materials including validations, applications and opportunities. Cem Concr Res. 2017;102:68–89.
[57] Sun H. Ab initio calculations and force field development for computer simulation of polysilanes. Macromolecules. 1995;28:701–12.
[58] van Duin ACT, Dasgupta S, Lorant F, Goddard WA. ReaxFF: A reactive force field for hydrocarbons. J Phys Chem A. 2001;105:9396–409.
[59] Manzano H, Pellenq RJM, Ulm F-J, Buehler MJ, van Duin ACT. Hydration of calcium oxide surface predicted by reactive force field molecular dynamics. Langmuir. 2012;28:4187–97.
[60] Manzano H, Masoero E, Lopez-Arbeloa I, Jennings HM. Shear deformations in calcium silicate hydrates. Soft Matter. 2013;9:7333–41.
[61] Yu Z, Lau D. Nano- and mesoscale modeling of cement matrix. Nanoscale Res Lett. 2015;10:173.
[62] Ebrahimi D, Whittle AJ, Pellenq RJM. Mesoscale properties of clay aggregates from potential of mean force representation of interactions between nanoplatelets. J Chem Phys. 2014;140:154309.
[63] Kalinichev AG, Wang J, Kirkpatrick RJ. Molecular dynamics modeling of the structure, dynamics and energetics of mineral–water interfaces: Application to cement materials. Cem Concr Res. 2007;37:337–47.
[64] Wang J, Wang Y, Wang R, Li W, Xu Y. Creep behavior of graphene oxide reinforced cement composites: Experiments, numerical simulations, and prediction models. Struct Concr. 2023;24:5441–50.
[65] Wang Q, Yue Q, Zhou W, Feng YT, Chang X. Modeling of both tensional-shear and compressive-shear fractures by a unified phase-field model. Appl Math Model. 2023;117:162–96.
[66] Wang Q, Yue Q, Huang C, Zhou W, Chang X. An adaptive local algorithm for solving the phase-field evolution equation in the phase-field model for fracture. Comput Mater Sci. 2022;214:111747.
[67] Yue Q, Zhou W, Wang Q, Feng YT, Ma G, Chang X. An adaptive phase-field model based on bilinear elements for tensile-compressive-shear fracture. Comput Math Appl. 2022;105:112–35.
[68] Wang Q, Feng YT, Zhou W, Cheng Y, Ma G. A phase-field model for mixed-mode fracture based on a unified tensile fracture criterion. Comput Methods Appl Mech Eng. 2020;370:113270.
[69] Yang H, Cui H, Tang W, Li Z, Han N, Xing F. A critical review on research progress of graphene/cement based composites. Compos Part A: Appl Sci Manuf. 2017;102:273–96.
[70] Lin C, Wei W, Hu YH. Catalytic behavior of graphene oxide for cement hydration process. J Phys Chem Solids. 2016;89:128–33.
[71] Fan D, Lue L, Yang S. Molecular dynamics study of interfacial stress transfer in graphene-oxide cementitious composites. Comput Mater Sci. 2017;139:56–64.
[72] Wan H, Zhang Y. Interfacial bonding between graphene oxide and calcium silicate hydrate gel of ultra-high performance concrete. Mater Struct. 2020;53:34.
[73] Hou D, Yang Q, Jin Z, Wang P, Wang M, Wang X, et al. Enhancing interfacial bonding between epoxy and CSH using graphene oxide: An atomistic investigation. Appl Surf Sci. 2021;568:150896.
[74] Lu Z, Yu J, Yao J, Hou D. Experimental and molecular modeling of polyethylene fiber/cement interface strengthened by graphene oxide. Cem Concr Compos. 2020;112:103676.
[75] Tran V-T, Nguyen T-K, Nguyen-Xuan H, Abdel Wahab M. Vibration and buckling optimization of functionally graded porous microplates using BCMO-ANN algorithm. Thin-Walled Struct. 2023;182:110267.
[76] Cuong-Le T, Nguyen KD, Hoang-Le M, Sang-To T, Phan-Vu P, Wahab MA. Nonlocal strain gradient IGA numerical solution for static bending, free vibration and buckling of sigmoid FG sandwich nanoplate. Phys B: Condens Matter. 2022;631:413726.
[77] Thanh CL, Nguyen TN, Vu TH, Khatir S, Abdel Wahab M. A geometrically nonlinear size-dependent hypothesis for porous functionally graded micro-plate. Eng Computers. 2022;38:449–60.
[78] Cuong-Le T, Hoang-Le M, Ferreira AJM, Abdel Wahab M. Small size-effect isogeometric analysis for linear and nonlinear responses of porous metal foam microplate. Compos Struct. 2022;285:115189.
[79] Du H, Pang SD. Enhancement of barrier properties of cement mortar with graphene nanoplatelet. Cem Concr Res. 2015;76:10–9.
[80] Tong T, Fan Z, Liu Q, Wang S, Tan S, Yu Q. Investigation of the effects of graphene and graphene oxide nanoplatelets on the micro- and macro-properties of cementitious materials. Constr Build Mater. 2016;106:102–14.
[81] Jorgensen WL, Tirado-Rives J. The OPLS [optimized potentials for liquid simulations] potential functions for proteins, energy minimizations for crystals of cyclic peptides and crambin. J Am Chem Soc. 1988;110:1657–66.
[82] Tersoff J. Empirical interatomic potential for carbon, with applications to amorphous carbon. Phys Rev Lett. 1988;61:2879–82.

[83] Lushnikova A, Zaoui A. Improving mechanical properties of C-S-H from inserted carbon nanotubes. J Phys Chem Solids. 2017;105:72–80.
[84] Hou D, Yang T, Tang J, Li S. Reactive force-field molecular dynamics study on graphene oxide reinforced cement composite: functional group de-protonation, interfacial bonding and strengthening mechanism. Phys Chem Chem Phys. 2018;20:8773–89.
[85] Sindu BS, Sasmal S. Molecular dynamics simulations for evaluation of surfactant compatibility and mechanical characteristics of carbon nanotubes incorporated cementitious composite. Constr Build Mater. 2020;253:119190.
[86] Merodio-Perea RG, Páez-Pavón A, Lado-Touriño I. Reinforcing cement with pristine and functionalized carbon nanotubes: experimental and simulation studies. Int J Smart Nano Mater. 2020;11:370–86.
[87] Verlet L. Computer "experiments" on classical fluids. I. thermodynamical properties of Lennard-Jones Molecules. Phys Rev. 1967;159:98–103.
[88] Zhao L, Nasution MKM, Hekmatifar M, Sabetvand R, Kamenskov P, Toghraie D, et al. The improvement of mechanical properties of conventional concretes using carbon nanoparticles using molecular dynamics simulation. Sci Rep. 2021;11:20265.
[89] Papanikolaou I, Al-Tabbaa A, Goisis M. An industry survey on the use of graphene-reinforced concrete for self-sensing applications. International Conference on Smart Infrastructure and Construction; 2019. p. 613–22.
[90] Zeng H, Qu S, Tian Y, Hu Y, Li Y. Recent progress on graphene oxide for next-generation concrete: Characterizations, applications and challenges. J Build Eng. 2023;69:106192.
[91] Zhang Y, Wang Q, Chen J, Tang J, Zhou H, Zhou W, et al. Preparation and performance study of active chemicals in cementitious capillary crystalline waterproofing materials. Case Stud Constr Mater. 2024;20:e02874.
[92] Zhong R, Ai X, Pan M, Yao Y, Cheng Z, Peng X, et al. Durability of micro-cracked UHPC subjected to coupled freeze-thaw and chloride salt attacks. Cem Concr Compos. 2024;148:105471.
[93] Zhong R, Zhang F. Engineering high-performance cementitious matrices for improved projectile impact resistance with silane, micro fibrillated cellulose and fine calcined bauxite aggregate. Cem Concr Compos. 2023;135:104835.
[94] Zhong R, Wille K. Deterioration of residential concrete foundations: The role of pyrrhotite-bearing aggregate. Cem Concr Compos. 2018;94:53–61.
[95] García-Macías E, Castro-Triguero R, Sáez A, Ubertini F. 3D mixed micromechanics-FEM modeling of piezoresistive carbon nanotube smart concrete. Comput Methods Appl Mech Eng. 2018;340:396–423.
[96] Yue Q, Wang Q, Zhou W, Rabczuk T, Zhuang X, Liu B, et al. An efficient adaptive length scale insensitive phase-field model for three-dimensional fracture of solids using trilinear multi-node elements. Int J Mech Sci. 2023;253:108351.
[97] Fouaidi M, Jamal M, Zaite A, Belouaggadia N. Bending analysis of functionally graded graphene oxide powder-reinforced composite beams using a meshfree method. Aerosp Sci Technol. 2021;110:106479.
[98] Nitka M, Tejchman J. A three-dimensional meso-scale approach to concrete fracture based on combined DEM with X-ray μCT images. Cem Concr Res. 2018;107:11–29.
[99] Ranjbarnia M, Zaheri M, Dias D. Three-dimensional finite difference analysis of shallow sprayed concrete tunnels crossing a reverse fault or a normal fault: A parametric study. Front Struct Civ Eng. 2020;14:998–1011.
[100] Huang X, Kong X, Chen Z, Fang Q. Peridynamics modelling of dynamic tensile failure in concrete. Int J Impact Eng. 2021;155:103918.
[101] Ghezelbash G, Babaelahi M, Saadatfar M. New analytical solution and optimization of a thermocline solar energy storage using differential quadrature method and genetic programming. J Energy Storage. 2022;52:104806.
[102] Andreaus U, Casini P, Vestroni F. Non-linear dynamics of a cracked cantilever beam under harmonic excitation. 2007;42:566–75.
[103] Saleh AL, Aliabadi MH. Crack growth analysis in concrete using boundary element method. Eng Fract Mech. 1995;51:533–45.
[104] Yue Q, Wang Q, Tian W, Rabczuk T, Zhou W, Ma G, et al. A phase-field lattice model (PFLM) for fracture problem: Theory and application in composite materials. Compos Struct. 2023;323:117432.
[105] Zaid O, Hashmi SRZ, Aslam F, Abedin ZU, Ullah A. Experimental study on the properties improvement of hybrid graphene oxide fiber-reinforced composite concrete. Diam Relat Mater. 2022;124:108883.
[106] Gallyamov ER, Cuba Ramos AI, Corrado M, Rezakhani R, Molinari JF. Multi-scale modelling of concrete structures affected by alkali-silica reaction: Coupling the mesoscopic damage evolution and the macroscopic concrete deterioration. Int J Solids Struct. 2020;207:262–78.
[107] Anastopoulos S, Givannaki F, Papanikos P, Metaxa Z, Alexopoulos ND. Calculation of a composite material's modulus of elasticity: comparison of results using fixed angles orientation and RVE with those using random orientation tensor and multi-step homogenization. Procedia Struct Integr. 2020;28:2132–41.
[108] Santhosi BVSRN, Ramji K, Rao NBRM, Nagaraju D, Naidu MK. Microwave absorption analysis of graphene-based hybrid nanocomposites: experimental, numerical and component level testing studies. Plast, Rubber Compos. 2023;52:129–44.
[109] Le J-L, Du H, Pang SD. Use of 2D graphene nanoplatelets (Gnp) in cement composites for structural health evaluation. Compos Part B: Eng. 2014;67:555–63.
[110] De Maio U, Fantuzzi N, Greco F, Leonetti L, Pranno A. Failure analysis of ultra high-performance fiber-reinforced concrete structures enhanced with nanomaterials by using a diffuse cohesive interface approach. 2020;10:1792.
[111] Pranno A, Greco F, Leonetti L, Lonetti P, Blasi PN, De Maio U. Cracking analysis in ultra-high-performance fiber-reinforced concrete with embedded nanoparticles via a diffuse interface approach. Procedia Struct Integr. 2022;39:688–99.
[112] Abdulkadir I, Mohammed BS, Liew MS, Wahab MMA. Modelling and optimization of the impact resistance of graphene oxide modified crumb rubber-ECC using response surface methodology. IOP Conference Series: Materials Science and Engineering. Vol. 1197; 2021. p. 012043
[113] Adamu M, Trabanpruek P, Jongvivatsakul P, Likitlersuang S, Iwanami M. Mechanical performance and optimization of high-volume fly ash concrete containing plastic wastes and graphene nanoplatelets using response surface methodology. Constr Build Mater. 2021;308:125085.
[114] Krystek M, Szojda L, Górski M. Numerical modelling of cement-graphene composites. Proceedings of the 12th fib International PhD Symposium in Civil Engineering; 2018. Prague, Czech Republic.

[115] Acar V, Cakir F, Uysal H, Seydibeyoglu MO, Akbulut H, Mosalam KM. Strengthening of concrete beams by monolayer prepreg composites with and without graphene reinforcement. Constr Build Mater. 2017;151:866–80.
[116] Ali Jafarian A, Reza K. Buckling analysis of embedded concrete columns armed with carbon nanotubes. Comput Concr. 2016;17:567–78.
[117] Bacciocchi M, Tarantino AM. Modeling and numerical investigation of the viscoelastic behavior of laminated concrete beams strengthened by CFRP strips and carbon nanotubes. Constr Build Mater. 2020;233:117311.
[118] Chan LY, Andrawes B. Characterization of the uncertainties in the constitutive behavior of carbon nanotube/cement composites. Sci Technol Adv Mater. 2009;10:045007.
[119] Sasmal S, Sindu BS, Gopinath S, Iyer NR. Numerical simulation of CNT incorporated cement. International Conference on Civil and Construction Technology; 2012.
[120] Sindu BS, Sasmal S. Properties of carbon nanotube reinforced cement composite synthesized using different types of surfactants. Constr Build Mater. 2017;155:389–99.
[121] Ghazizadeh S, Duffour P, Skipper NT, Billing M, Bai Y. An investigation into the colloidal stability of graphene oxide nano-layers in alite paste. Cem Concr Res. 2017;99:116–28.
[122] Zhang H, Huang YJ, Yang ZJ, Xu SL, Chen XW. A discrete-continuum coupled finite element modelling approach for fibre reinforced concrete. Cem Concr Res. 2018;106:130–43.
[123] Pranno A, Greco F, Leonetti L, Lonetti P, Blasi PN, De Maio U. Cracking analysis in ultra-high-performance fiber-reinforced concrete with embedded nanoparticles via a diffuse interface approach. 2022;39:688–99.
[124] De Sukrit K, Mukherjee A. A numerical model for electrical properties of self-sensing concrete with carbon fibers. J Mater Civ Eng. 2023;35:04023311.
[125] Mortazavi B, Benzerara O, Meyer H, Bardon J, Ahzi S. Combined molecular dynamics-finite element multiscale modeling of thermal conduction in graphene epoxy nanocomposites. Carbon. 2013;60:356–65.
[126] Park HS, Liu WK. An introduction and tutorial on multiple-scale analysis in solids. Comput Methods Appl Mech Eng. 2004;193:1733–72.
[127] Ulz MH. Coupling the finite element method and molecular dynamics in the framework of the heterogeneous multiscale method for quasi-static isothermal problems. J Mech Phys Solids. 2015;74:1–18.
[128] Chandra Y, Adhikari S, Saavedra Flores EI, Figiel Ł. Advances in finite element modelling of graphene and associated nanostructures. Mater Sci Eng: R: Rep. 2020;140:100544.
[129] Wei X, Kysar JW. Experimental validation of multiscale modeling of indentation of suspended circular graphene membranes. Int J Solids Struct. 2012;49:3201–9.
[130] Montazeri A, Naghdabadi R. Investigation of the interphase effects on the mechanical behavior of carbon nanotube polymer composites by multiscale modeling. J Appl Polym Sci. 2010;117:361–7.
[131] Chandra Y, Scarpa F, Adhikari S, Zhang J, Saavedra Flores EI, Peng H-X. Pullout strength of graphene and carbon nanotube/epoxy composites. Compos Part B: Eng. 2016;102:1–8.
[132] Chandra Y, Saavedra Flores EI, Scarpa F, Adhikari S. Buckling of hybrid nanocomposites with embedded graphene and carbon nanotubes. Phys E. 2016;83:434–41.
[133] Rafiee R, Eskandariyun A. Estimating Young's modulus of graphene/polymer composites using stochastic multi-scale modeling. Compos Part B: Eng. 2019;173:106842.
[134] Rafiee R, Eskandariyun A. Predicting Young's modulus of agglomerated graphene/polymer using multi-scale modeling. Compos Struct. 2020;245:112324.
[135] Guo Z, Song L, Chai GB, Li Z, Li Y, Wang Z. Multiscale finite element analyses on mechanical properties of graphene-reinforced composites. Mech Adv Mater Struct. 2019;26:1735–42.
[136] Li C, Chou T-W. Multiscale modeling of compressive behavior of carbon nanotube/polymer composites. Compos Sci Technol. 2006;66:2409–14.
[137] Chandra Y, Scarpa F, Chowdhury R, Adhikari S, Sienz J. Multiscale hybrid atomistic-FE approach for the nonlinear tensile behaviour of graphene nanocomposites. Compos Part A: Appl Sci Manuf. 2013;46:147–53.
[138] Chandra Y, Chowdhury R, Scarpa F, Adhikari S, Sienz J, Arnold C, et al. Vibration frequency of graphene based composites: A multiscale approach. Mater Sci Eng, B. 2012;177:303–10.
[139] Thilakarathna PSM, Kristombu Baduge KS, Mendis P, Lee H, Chandrathilaka ERK, Vimonsatit V. Multiscale modelling framework for elasticity of ultra high strength concrete using nano/microscale characterization and finite element representative volume element analysis. Constr Build Mater. 2022;327:126968.
[140] Papadopoulos V, Seventekidis P, Sotiropoulos G. Stochastic multiscale modeling of graphene reinforced composites. Eng Struct. 2017;145:176–89.
[141] Li C, Chou T-W. A structural mechanics approach for the analysis of carbon nanotubes. Int J Solids Struct. 2003;40:2487–99.
[142] Li C, Chou TW. Multiscale modeling of carbon nanotube reinforced polymer composites. J Nanosci Nanotechnol. 2003;3:423–30.
[143] Giannopoulos GI, Kakavas PA, Anifantis NK. Evaluation of the effective mechanical properties of single walled carbon nanotubes using a spring based finite element approach. Comput Mater Sci. 2008;41:561–9.
[144] Rafiee R, Eskandariyun A. Comparative study on predicting Young's modulus of graphene sheets using nano-scale continuum mechanics approach. Phys E. 2017;90:42–8.
[145] Scarpa F, Adhikari S, Srikantha Phani A. Effective elastic mechanical properties of single layer graphene sheets. Nanotechnology. 2009;20:065709.
[146] Bakshi SR, Patel RR, Agarwal A. Thermal conductivity of carbon nanotube reinforced aluminum composites: A multi-scale study using object oriented finite element method. Comput Mater Sci. 2010;50:419–28.
[147] Liu JZ, Zheng Q, Jiang Q. Effect of a rippling mode on resonances of carbon nanotubes. Phys Rev Lett. 2001;86:4843–6.
[148] Arroyo M, Belytschko T. An atomistic-based finite deformation membrane for single layer crystalline films. J Mech Phys Solids. 2002;50:1941–77.
[149] Pantano A, Boyce MC, Parks DM. Nonlinear structural mechanics based modeling of carbon nanotube deformation. Phys Rev Lett. 2003;91:145504.
[150] Hemmasizadeh A, Mahzoon M, Hadi E, Khandan R. A method for developing the equivalent continuum model of a single layer graphene sheet. Thin Solid Films. 2008;516:7636–40.
[151] Chen XL, Liu YJ. Square representative volume elements for evaluating the effective material properties of carbon nanotube-based composites. Comput Mater Sci. 2004;29:1–11.

[152] Namilae S, Chandra N. Multiscale model to study the effect of interfaces in carbon nanotube-based composites. J Eng Mater Technol. 2005;127:222–32.
[153] Wang X, Wang XY, Xiao J. A non-linear analysis of the bending modulus of carbon nanotubes with rippling deformations. Compos Struct. 2005;69:315–21.
[154] Wan H, Delale F, Shen L. Effect of CNT length and CNT-matrix interphase in carbon nanotube (CNT) reinforced composites. Mech Res Commun. 2005;32:481–9.
[155] Liu YJ, Chen XL. Evaluations of the effective material properties of carbon nanotube-based composites using a nanoscale representative volume element. Mech Mater. 2003;35:69–81.
[156] Nasdala L, Ernst G. Development of a 4-node finite element for the computation of nano-structured materials. Comput Mater Sci. 2005;33:443–58.
[157] Nasdala L, Kempe A, Rolfes R. Are finite elements appropriate for use in molecular dynamic simulations? Compos Sci Technol. 2012;72:989–1000.
[158] Eftekhari M, Mohammadi S. Multiscale dynamic fracture behavior of the carbon nanotube reinforced concrete under impact loading. Int J Impact Eng. 2016;87:55–64.
[159] Rupasinghe M, Mendis P, Ngo T, Nguyen TN, Sofi M. Compressive strength prediction of nano-silica incorporated cement systems based on a multiscale approach. Mater Des. 2017;115:379–92.
[160] Eftekhari M, Mohammadi S, Khanmohammadi M. A hierarchical nano to macro multiscale analysis of monotonic behavior of concrete columns made of CNT-reinforced cement composite. Constr Build Mater. 2018;175:134–43.
[161] Eftekhari M, Karrech A, Elchalakani M, Basarir H. Multi-scale modeling approach to predict the nonlinear behavior of CNT-reinforced concrete columns subjected to service loading. Structures. 2018;14:301–12.
[162] Negi A, Bhardwaj G, Saini JS, Khanna K, Godara RK. Analysis of CNT reinforced polymer nanocomposite plate in the presence of discontinuities using XFEM. Theor Appl Fract Mech. 2019;103:102292.
[163] Eftekhari M, Karrech A, Elchalakani M. Investigation into the nonlinear time-history analysis of CNT-reinforced concrete column by a multiscale approach. Int J Civ Eng. 2020;18:49–64.
[164] Liew KM, Pan Z, Zhang L-W. The recent progress of functionally graded CNT reinforced composites and structures. Sci China: Phys, Mech Astron. 2019;63:234601.
[165] Ahmadi M, Ansari R, Rouhi S. Response of graphene reinforced concrete to the external compressive load: A multiscale approach. Struct Concr. 2018;19:1702–12.
[166] Papadopoulos V, Impraimakis M. Multiscale modeling of carbon nanotube reinforced concrete. Compos Struct. 2017;182:251–60.
[167] Wang JF, Zhang LW, Liew KM. Multiscale simulation of mechanical properties and microstructure of CNT-reinforced cement-based composites. Comput Methods Appl Mech Eng. 2017;319:393–413.
[168] Montinaro N, Pantano A. Parameters influencing the stiffness of composites reinforced by carbon nanotubes – A numerical–analytical approach. Compos Struct. 2014;109:246–52.
[169] Bagherzadeh F, Shafighfard T. Ensemble machine learning approach for evaluating the material characterization of carbon nanotube-reinforced cementitious composites. Case Stud Constr Mater. 2022;17:e01537.
[170] Bishara D, Xie Y, Liu WK, Li S. A state-of-the-art review on machine learning-based multiscale modeling, simulation, homogenization and design of materials. Arch Computational Methods Eng. 2023;30:191–222.
[171] Unger JF, Könke C. Neural networks as material models within a multiscale approach. Comput Struct. 2009;87:1177–86.
[172] Rao C, Liu Y. Three-dimensional convolutional neural network (3D-CNN) for heterogeneous material homogenization. Comput Mater Sci. 2020;184:109850.
[173] Lyngdoh GA, Das S. Integrating multiscale numerical simulations with machine learning to predict the strain sensing efficiency of nano-engineered smart cementitious composites. Mater Des. 2021;209:109995.
[174] Lu X, Giovanis DG, Yvonnet J, Papadopoulos V, Detrez F, Bai J. A data-driven computational homogenization method based on neural networks for the nonlinear anisotropic electrical response of graphene/polymer nanocomposites. Comput Mech. 2019;64:307–21.
[175] Wang W, Chen SJ, Duan W, Sagoe-Crentsil K, Pathirage CSN, Li L, et al. Revealing microstructural modifications of graphene oxide-modified cement via deep learning and nanoporosity mapping: implications for structural materials' performance. ACS Appl Nano Mater. 2022;5:7092–102.
[176] Tong Z, Guo H, Gao J, Wang Z. A novel method for multi-scale carbon fiber distribution characterization in cement-based composites. Constr Build Mater. 2019;218:40–52.
[177] Huang JS, Liew JX, Liew KM. Data-driven machine learning approach for exploring and assessing mechanical properties of carbon nanotube-reinforced cement composites. Compos Struct. 2021;267:113917.